Kinetic and thermodynamic study of composite with jute fiber as reinforcement

Edja Florentin Assanvo[a*] [iD], Kicoun Jean-Yves N'Zi Toure[a,b,c] [iD], Kanga Marius N'Gatta [a], David Boa[a] [iD]

[a] *Laboratoire de Thermodynamique et Physico-Chimie des Matériaux, Université Nangui Abrogoua, Abidjan, Côte d'Ivoire*

[b] *Department of Physics, Kenyatta University P.O.BOX 43844-00100, Nairobi, Kenya*

[c] *Department of Physics, Worcester Polytechnic Institute 100 Institute Road, Worcester MA, 01609-2280, United States of America*

Abstract. In the present work, engineered by compression molding process via a hydraulic press, the A and B composite samples were carried out with 5% and 10% ratio respectively of *Ricinodendron heudelotii* oil-based alkyd resin in bio-based matrix made of unsaturated polyester using jute fibers as reinforcement material. The samples' thermal decomposition was performed through thermogravimetry (TG) and derivative thermogravimetry (DTG) analyses. Both composite samples exhibit two stages of decomposition, where the main occurs at 200 - 550°C. Aiming to study and being able to model the thermal degradation of the elaborated composites, finding the kinetic triplets appears the best option to describe the kinetic process undergo by the composites in order to evaluate the performance application of the composites. Two non-isothermal techniques, Flynn-Wall-Ozawa (FWO) and Kissinger have been used to assess the activation energy-Ea, and it is found that the apparent activation energy varies with the degree of conversion indicating that both composites decompose with a multiple step mechanism process. The appropriate reaction model for the second stage of decomposition was best suited with Johnson-Mel-Avrami (n<1) model and has been established, allowing us to model thermal degradation behavior of our elaborated composite material and set predictions. The estimated Arrhenius factor values were respectively about A and B composites, $4.12.10^{15}$ min^{-1} and $10.42.10^{15}$ min^{-1}, allowing us to set the final equation characterizing the degradation process for the second and main decomposition stage. Finally, as a result of comparison between A and B composites, A appears to be the more thermally stable due to its lower values of Arrhenius pre-exponential factor over the main stage of decomposition and higher calculated the activation energy values.

Keywords: Natural Fiber, Activation energy, Thermal degradation, Kinetic model, Thermal modelling.

1. Introduction

Research into the creation of novel green bio-based and biodegradable materials from natural resources for various engineering applications has been stimulated by a growing concern for environmental preservation. In fact, the availability, affordability, and numerous other benefits of natural resources make them attractive for their use in the engineering of these novel types of materials (La Mantia & Morreale, 2011; Mugdha Bhat *et al.*, 2021; Scatolino *et al.*, 2017). As an alternative to customary plastic made from petroleum, a lot of conducted studies were done on the utilization of natural lignocellulosic fibers (NLF) to create more valuable materials in a sustainable and ecologically acceptable manner that may be used in a variety of industrial applications. The possible use of lignocellulosic materials as sources of reinforcing fillers for thermoplastic and thermosetting biopolymers has also been investigated by number of researchers (Kakati *et al.*, 2019; Kuranchie *et al.*, 2021; R. H. M. Reis *et al.*, 2020; R. S. Reis *et al.*, 2020). One key strategy aiming to avoid the complexity of recycling is the use of naturally disintegrating materials after usage. In order to enhance composite materials properties, researchers have since developed the incorporation of natural

fibers (NF) for instance hemp (Khoathane *et al.*, 2008; Oza *et al.*, 2014), flax (Zafeiropoulos *et al.*, 2002), sisal (Khoathane *et al.*, 2008), coconut (Rosa *et al.*, 2009), kenaf (Hamidon *et al.*, 2019), pineapple leaf (Kakati, 2019), and more in their elaboration (Arrakhiz *et al.*, 2013; Sahin *et al.*, 2017; Scatolino *et al.*, 2017). Although these materials are in demand in many sectors, such as automobile, sport, aviation, building…, where materials must be preserved over the time, exposed to light or sunlight, heat and humidity. The significance of NF composites lies in their sustainability, renewability and potential to reduce environmental impact compared to the traditional synthetic fiber composites (Butler, S. (2018); Barsoum, 2019; Keller, 2003; Kuranchie *et al.*, 2021; La Mantia & Morreale, 2011; Raju & Kumarappa, 2012; R. H. M. Reis *et al.*, 2020; R. S. Reis *et al.*, 2020; Yakout & Elbestawi, 2017). However, it's important to note that they are subjected to limitations in terms of moisture absorption, dimensional stability, mechanical properties. The poor adhesion fiber/matrix compatibility mainly come from the hydrophilic property of the fiber and the hydrophobicity of the used matrix (Tserki *et al.*, 2005; Zafeiropoulos *et al.*, 2002), moreover, the undesired compounds of the fibers including hemicellulose and lignin. The use of untreated fibers may lead

* Corresponding author
Email: aedjaflorentin@gmail.com (E.F.Assanvo)

E.F.Assanvo et al

Int. J. Renew. Energy Dev 2024, 13(1), 1-9

| 2

to composite materials with low properties due to the NF drawbacks. It would be important to carry out more in-depth studies in order to optimize their use and properties related to the different conditions.

Among all existing natural fibers today, jute looks to be one of the NF employed more frequently as reinforcement in green composites, and presently, bast fibers with the highest global output volume (Singh *et al.*, 2018; Thiruchitrambalam *et al.*, 2010). Jute chemical composition is in the range of 45-73.2% cellulose, 12-24% hemicellulose, 5-25% lignin, and properties including tensile strength (300-800Mpa), Young's modulus (2.5-55Gpa), elongation at break (1-4%) and density (1.3-1.46g/cm3) according to the review of the study of Singh *et al.*, 2018, allowing good specifications to be used to strengthen composite materials. In fact, using jute fibers in order to create composite materials result in materials that have good thermal properties (Rangappa, 2021), mechanical properties (Nenonene, 2014; R. H. M. Reis *et al.*, 2020), rheology properties (Elisabeth *et al.*, 2018), and optical properties (N'Gatta *et al.*, 2022), which are suitable for application in various domains. Despite the fact that jute fiber can deteriorate due to several factors including moisture and water damage, microbial attack, chemical degradation or under exposure to UV radiation, exploring the ways of proper handling techniques or fiber treatments will enhance the fiber properties and help reducing drawbacks on the use of jute fiber as reinforcement in composite materials elaboration.

Research on the use of jute fiber in composite materials application has been carried out up to now, and have shown good results depending on the application domain with the various treatments applied onto the fibers. The kinetic and thermodynamic investigation of the degradation of composite materials utilizing jute fiber as reinforcement, source of renewable material, however, has not yet been published. Moreover, extending the range of applications for renewable green composites requires an understanding of the kinetic mechanism and model as well as the thermal stability and deterioration processes. This work studied the kinetic analysis of the thermal degradation of green composites that were developed using jute fibers as reinforcement combine with a bio-based matrix, in order to create a completely biodegradable and environmentally friendly composite materials.

2. Materials and methods

2.1 Materials

Ricinodendron heudelotii (RH) oil-based alkyd resin (Assanvo *et al.*,2015), soy flour resin (SFR) (Kakati *et al.*, 2019), unwoven jutes sheets (arbitrary laying) and jute-fiber materials from the National Institute of Research on Jute and Allied Fibers Technology, Kolkata, India.
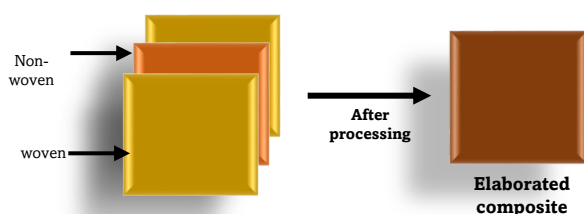

Fig. 1 Jute fiber layer disposition structure for the material elaboration

2.2 Bio-based matrix synthesis

Blends of bio-based unsaturated matrix resin were made in two sets, A and B. The first batch of blend A contains 5% i.e., 5 g RH oil-based alkyd resin in 100 g of SFR. While the second set B consists of 10% meaning 10 g of RH oil-based alkyd resin fraction in 100 g of SFR. For the preparation of the bio-based matrix blends, the RH oil-based alkyd and soy four resin were blended in a cone-shaped flask at room temperature for 2 hours at a high-speed agitator of 10,000 rpm.

2.3 Elaboration of jute fiber reinforced material with the bio-based unsaturated resin matrix

Using a PEECO PVT LTD Kolkata hydraulic press associated and by compression molding process, we managed to manufacture the A and B composite based on the prepared matrix, respectively. Non-woven and woven mats made with jute fibers were cut in 30cm×7cm dimension, and impregnated in the resin matrix. The excess resin was pressed out, and the impregnated jute mats were then allowed to dry for 24h at room temperature. Two 30cm×30cm×0.5cm steel plates were used for the composite's elaboration. Thin plastic layer of paper was inserted between the mats and the plates in order to obtain a good composite surface, then the dried carpets were placed alternately layer after layer (Figure 1) a total of 10 carpets of non-woven sheets and 9 woven sheets. Following that, the molds were hot-cured by compression in the hydraulic press for 15 minutes at 110°C and 200Kg/cm². After curing, the composite samples were taken out of the molds and desiccated to avoid moisture absorption.

2.4 TGA & DSC measurements

The thermal degradation and stability of the elaborated composite materials were determined using a DSC-TGA module instrument, TA STD series Q600 under an inert atmosphere (nitrogen gas) at 4 distinct thermal rates, 20, 15, 10 et 5°C/min. A mass of 6mg of crushed sample were taken in an alumina crucible, and subjected to a temperature program varying from 25°C to 600°C while performing the experiment. The nitrogen gas flow was 100 mL/min, and the analysis performed at North-East Institute of Science and Technology, Jorhat, India.

2.5 Thermal degradation theory

Investigation on the deterioration of polymeric materials is extremely beneficial in thermal degradation steps understanding, kinetic models and mechanisms, thermal steadiness and cycling. Kinetic analysis is critical because it gives information that can be utilized to optimize and/or improve process parameters, also to provide information on the mathematical modeling simplification (Khachani *et al.*, 2014). The apparent activation energy (E_α), frequency or Arrhenius pre-exponential factor (A), and the order of reaction (n) are the variables kinetic analysis. With the aim of examining the kinetics of the thermal deterioration processes and identify the characteristic variables such as $f(\alpha)$ and $g(\alpha)$ functions, the TG analysis approach has been widely employed (Assanvo *et al.*, 2015; Khachani *et al.*, 2014).

The temperature T and the degree of conversion α are two metrics widely used to display the reaction rate in a process as the recognized equation (1) where $f(\alpha)$ is the reaction model function which allows us to model the final equation characterizing the degradation process:

E.F.Assanvo et al

Int. J. Renew. Energy Dev 2024, 13(1), 1-9

| 3

$$\left(\frac{d\alpha}{dt}\right) = K(T).f(\alpha) \tag{1}$$

The rate or decomposition constant, $K(T)$, which is frequently parameterized by the Arrhenius equation (2), expresses the process rate's temperature dependence, and the heating rate β, which can be defined by equation (3):

$$K(T) = A\,exp\left(\frac{-E_a}{RT}\right) \tag{2}$$

$$\beta = \frac{dT}{dt} \tag{3}$$

where A is the pre-exponential factor (S^{-1}), E_a the activation energy $(KJ.mol^{-1})$, R the universal gas constant $(8.314\,J.mol^{-1}.K^{-1})$, and $T(K)$ the unconditional temperature. The reliance on the degree of conversion is shown by the reaction model function, $f(\alpha)$, that may be connected to the testing data. For data derived at steady heating rate, β and $K(T)$ are switched in equation (1) to get the equation (4):

$$\frac{d\alpha}{dT} = \frac{A}{\beta}.exp\left(\frac{-E_a}{RT}\right).f(\alpha) \tag{4}$$

It is feasible to evaluate $f(\alpha)$ with a basic model function for simple reactions. For complex reactions $f(\alpha)$ functions are sophisticated and usually undetermined; in this situation, the process of simple reaction guides to considerable discrepancies in kinetics data. It exists an integral kinetic method (advanced isoconversional method) developed by Vyazovkin et al., (2011). De facto, the relative involvement of each single-step process to the global reaction rate is what causes the change in activation energy with.

In the current work, two techniques were employed to evaluate the activation energy for the disintegration of our composite materials at various heating speeds: Kissinger and Flynn-Wall-Ozawa (FWO) techniques.

No matter how complex the process is, renowned for providing an unbeatably simple way of determining the activation energy and for drastically oversimplifying the kinetics of the phenomena it considers., the Kissinger technique (Vyazovkin, 2020) is a differential method that produce a single value for the activation energy. The activation energy, E, is calculated using the Kissinger equation in its most straightforward form:

$$E = -R\frac{d\ln\left(\frac{\beta}{T_m^2}\right)}{dT_m^{-1}} \tag{5}$$

where T_m is the temperature associated with the location of the rate peak maximum. The integral version of the Kissinger equation is more illuminating through equation (6) that derives from equation (5).

$$\ln\left(\frac{\beta}{T_m^2}\right) = \ln\left(-\frac{AR}{E}f'(\alpha_m)\right) - \frac{E}{RT_m} \tag{6}$$

According to both equations (5) and (6), the Kissinger plot's incline of $ln\left(\frac{\beta}{T_m^2}\right)$ can be utilized to figure out the activation energy.

The activation energy and pre-exponential factor are calculated using the FWO method, an isoconversional method. Furthermore, that method required the samples to be heated at

various temperature heating rate, minimum three different temperature programs. Using its final method equation (7), the slope of the plot line derived from various heating temperature rates can be used to solve for the activation energy. For each degree of conversion, this approach offers a different activation energy and pre-exponential factor value.

$$\log(\beta) = \log\left(\frac{AE}{R}\right) - \log(g(\alpha)) - 2,315 - 0.4567\frac{E_\alpha}{RT} \tag{7}$$

The real $f(\alpha)$, which must be invariant for all heating rates, is not necessary to use the isoconversional technique. Malek's approach, which suggests that the $f(\alpha)$ function are related to $y(\alpha)$ and $z(\alpha)$, can be used to investigate the invariance and is principally achieved by a straightforward TG data translation. Equations (8) and (9) represent these functions under non-isothermal conditions:

$$y(\alpha) = \left(\frac{d\alpha}{dt}\right)\exp\left(\frac{E_a}{RT}\right) = Af(\alpha) \tag{8}$$

$$z(\alpha) = \left(\frac{d\alpha}{dt}\right)T^2 = p\left(\frac{E}{RT}\right)\left(\frac{d\alpha}{dt}\right)\frac{T}{\beta} = f(\alpha).g(\alpha) \tag{9}$$

An overview of the of the mathematical characteristics of the $y(\alpha)$ and $z(\alpha)$ functions for typical kinetic models is given in the table of the fundamental kinetic models (see Table in annex) and attributes of these functions (Assanvo et al., 2015). Following by the identification of the reaction model, find the pre-exponential factor A to obtain the three key kinetic parameters, E_a, $f(\alpha)$ and A, follow the identification of the reaction model. From the Malek theory (MaÂlek, 2000), (Janković et al., 2008; Khachani et al., 2014), we derive A by the equation 10:

$$A = \frac{-\beta E_a}{RT_{max}^2\,f'(\alpha_{max})}\exp\left(\frac{E_a}{RT_{max}}\right) \tag{10}$$

Where $f'(\alpha_{max})$ is the derivative of the $f(\alpha)$ function from α_{max}, and T_{max}, α_{max} signify the maximum peak on the DTG curve.

3. Results and Discussions

The ICTAC Kinetic Committee's reliable isoconversional (model-free) method, which involves several temperature programs (Assanvo et al., 2015; Janković et al., 2008; Vyazovkin et al., 2011) were used to perform kinetic computations through thermal analysis data of A and B composites. Different constant heating rates were used during the trials, including $20, 15, 10$ and $5°C/min$. Figure 2 shows, the temperature at the four heating rates against the thermal analysis data (TGA and DTG) of A and B composites.

The TG curves in Figure 2 (a) and (c) show A and B composite samples decomposition with more than 20% residue formation. More precisely in the range gap of 25-30% and 20-25% for A and B composites respectively. At this condition, we can deduce that A contains more inorganic compounds than B composite (Tajvidi & Takemura, 2010). For both composites TG analysis at all various heating rates, a slight weight loss is observed below $100°C$ which is attributed to the evaporation of absorbed moisture. All formulation exhibits significant weight losses at any temperature as compare to the different heating rate processed where tiny differences are observed at each heating rate.
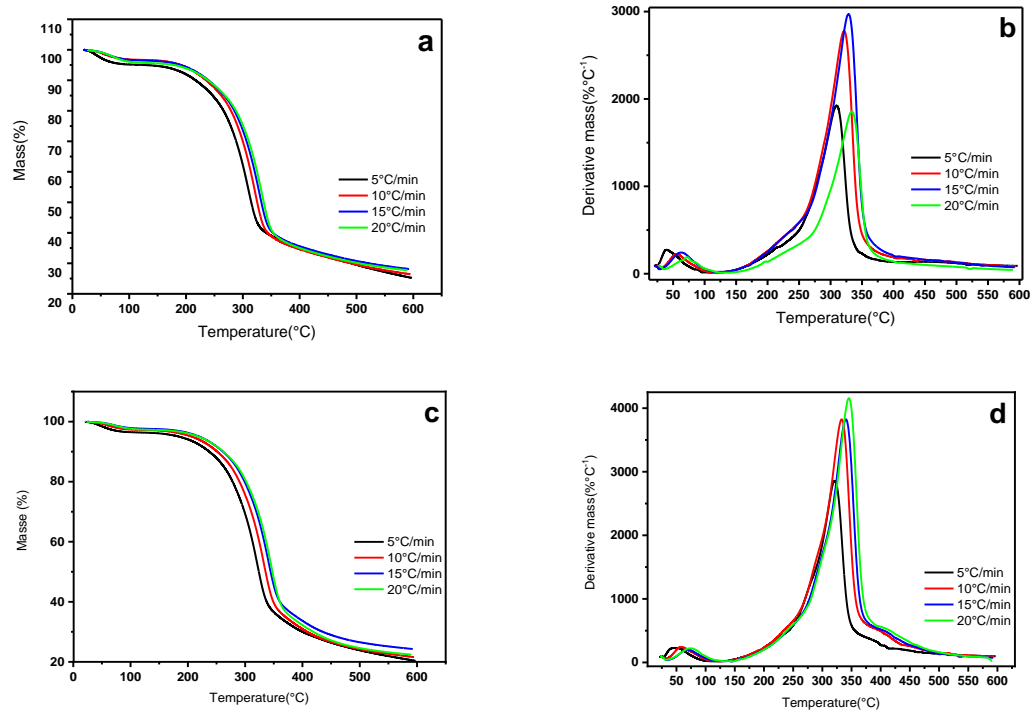
E.F.Assanvo et al   Int. J. Renew. Energy Dev 2024, 13(1), 1-9

| 4

Fig. 2 Composite A's TGA (a) and DTG (b) curves Composite B's TGA (c) and DTG (d) curves at 20, 15, 10 and 5°C/min β heating rate

The derivative curves in Figure 2 (b) and (d) reveal the same trend for all composite materials, which also shows that the maximum decomposition temperature rises as the heating rates rise. In addition, they also show two distinct stages of degeneration. The first stage of degradation happens in the range of 25-125°C and may be assigned to the gradual release of remaining water from the composites and the depolymerization process. The main degradation (second stage) occurs over a broader temperature range of 225-375 °C with mass loss of 9.01-60% at a relatively high temperature with maximum temperature at approximatively 333 °C. This high temperature decomposition is attributed to the decomposition of lignocellulosic fibers by the decomposition of hemicelluloses which are the least thermally stable lignocellulosic components, cleavage of glycosidic linkage of cellulose as well as the disintegration of the crosslinking lattice formed between the matrix and the fibers (Monteiro *et al*., 2012; Darus *et al*., 2020).

Utilizing the Kissinger (differential) and FWO (integral) approaches, the activation energy values calculated and reported in, Table 1 were in good agreement, demonstrating good convergence between the two methods. Figure 3 depicts the linear plot of the Kissinger technique for the composites A and B for the main stage of decomposition.

The isoconversional Flynn-Wall-Ozawa method lines for both composites and decomposition stages are shown in Figure 4. Figure 4(a) and (c) show that the isoconversional plot for the first stage of decomposition, and it is clearly shown that, the fitted lines are non-parallel indicating a complex degradation mechanism. On the other hand, case of the second decomposition stage as shown in Figure 4(b) and (d), the adjusted lines are almost parallel, thus giving two possibilities of decomposition mechanisms. A single mechanism underlies the decomposition reaction if the lines are parallel, or at least two stages and a more complex mechanism if the lines are not
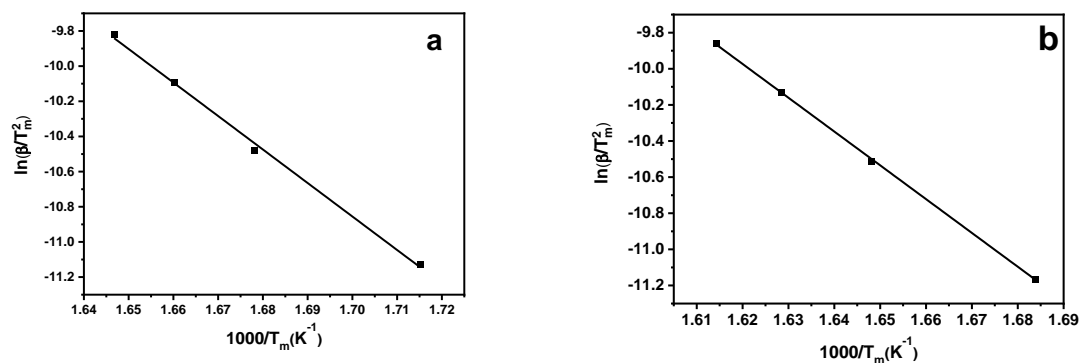

Fig. 3 Kissinger plot of composites A(a) and B(b) second stage of decomposition

E.F.Assanvo et al   *Int. J. Renew. Energy Dev 2024, 13(1), 1-9*

|5

Table 1

Activation energies for different stages of decomposition for A and B composites

Conversion α	Composite A				Composite B			
	Kissinger		Flynn-Wall-Ozawa		Kissinger		Flynn-Wall-Ozawa	
	$E_\alpha(Kj. mol^{-1})$	r^2	$E_\alpha(Kj. mol^{-1})$	r^2	$E_\alpha(Kj. mol^{-1})$	r^2	$E_\alpha(Kj. mol^{-1})$	r^2
First stage								
0.03			32.12	0.961			35.99	0.954
0.04			34.02	0.972			30.84	0.956
0.05			33.71	0.957			39.36	0.973
Mean	32.80	0.989	32.28		37.70	0.930	35.40	
Second stage								
0.2			122.03	0.960			146.41	0.996
0.3			168.12	0.985			158.58	0.992
0.4			174.28	0.996			166.62	0.999
0.5			182.38	0.999			172.50	0.999
0.6			189.10	0.999			178.81	0.999
0.7			202.16	0.998			189.43	0.999
Mean	168.40	0.996	173.01		165,59	0.999	168.72	

parallel. The investigation on the relationship between the activation energy and the degree of conversion (α) is a useful tool to know the degradation mechanism of the main stage. According to the solution of equation (6) and (7) and the table 1, the activation energy, which is the minimal amount of energy needed to start our composites' degradation reaction process

(Hadiyanto *et al.*, 2018), and in fact also related to the reactional material stability. Results show that the energy activation values increase as the degree of conversion increases. The activation energy's relationship to the degree of conversion suggests that the thermal disintegration of composites A and B is the result of a complex reaction process. This degradation mechanism clue
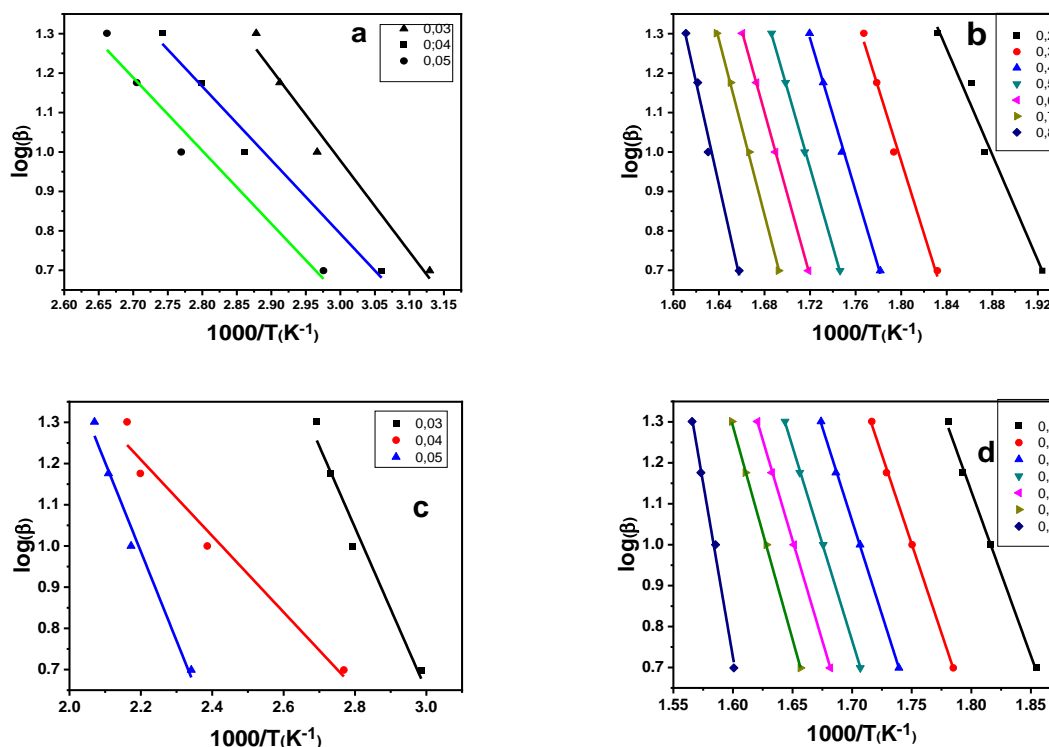

Fig. 4 Iso-conversion plot using the F–W–O method with varied degrees of conversions of composite A first (a) and second stage (b); and composite B first (c) and second stage (d).

E.F.Assanvo et al

Int. J. Renew. Energy Dev 2024, 13(1), 1-9

| 6

can be attributed to crosslinking complex reaction associated with vitrification and debonding of the cellulosic-matrix link prior decomposition.

The activation energy of the composite A is higher than of the composite B (Table 1) indicating that as the percentage of resin modifier increases, this could lead increasingly low E_α values resulting to a less and less stable composite material. These findings also imply that the inclusion of resin modifier can reduce the adherence of the fiber matrix. This information is crucial since A composite is probably more thermally stable than B.

The method put worth by Malek (MaÂlek, 2000) and the recommendations given by the ICTAC Kinetic Committee (Vyazovkin *et al.*, 2011) were both used to determine which kinetic model for non-isothermal deterioration of the two composites better fit the experimental results. The normalized graphs of $y(\alpha)$ and $z(\alpha)$ functions are shown in Figure 5, and the curves show no significant with the given β values. $\alpha_{max,z}$ values obtained from the curves are 0.660 and 0.632 respectively for the composites A and B. $y(\alpha)$ function presents a concave behavior for both composites and exhibit a maximum $\alpha_{max,z}$ corresponding the model describes Johnson-Mel-Avrami (JMA). According to Svoboda & Málek, (2011), the value of n are calculated using $\alpha_{max,y}$.

Calculated n values are $n = 0.48$ and $n = 0.5$ respectively for A and B composites. In the α-range of 0.2 to 0.7, the kinetic reaction models for A and B composites degradation are established as follow:

- Composite A: $f_A(\alpha) = 0.48(1-\alpha)[-\ln(1-\alpha)]^{(-1.08)}$ (11)

- Composite B: $f_B(\alpha) = 0.5(1-\alpha)[-\ln(1-\alpha)]^{(-1)}$ (12)

For JMA model; randomization (random distribution) is implemented by $(1-1/n) = 1$, $(1-1/n) > 1$ or an orderly distribution, and finally $(1-1/n) < 1$ for a bundled distribution, then the composites degrade in a grouped way regarding their n calculated values.

After being calculated, the $f'(\alpha_{max})$ and Arrhenius factor A are recorded in Table 2 for A and B composites respectively, and their mean Arrhenius pre-exponential factor value were shown to be:

- Composite A: $A = 4.12*10^{15} min^{-1}$;
- Composite B: $A = 10.42*10^{15} min^{-1}$.

As a result, from all above, the kinetic triplets E_α, A and $f(\alpha)$ are well known. For the second and main degradation step, the final equation characterizing the degradation of A and B composites is established by:

- Composite A:

$$\beta\frac{d\alpha}{dT} = 4.12*10^{15}\exp\left(\frac{173.01}{RT}\right)*0.48(1-\alpha)[-\ln(1-\alpha)]^{(-1.08)} \quad (13)$$

- Composite B

$$\beta\frac{d\alpha}{dT} = 10.42*10^{15}\exp\left(\frac{168.72}{RT}\right)*0.5(1-\alpha)[-\ln(1-\alpha)]^{(-1)} \quad (14)$$

After deduction regarding the analyses made above, the reaction model found to be ideal for the description of the decomposition of both composites is that of JMA with a value of n less than 1 describing a bundled distribution. Based on the different TGA and DTG curves observed and after analysis, composites A and B exhibit the same trend of thermal degradation process, with two decomposition steps showing that both composites describe the same thermal behavior. The frequency factor, or Arrhenius factor value, which describes how frequently two molecules collide, appears to be lower for
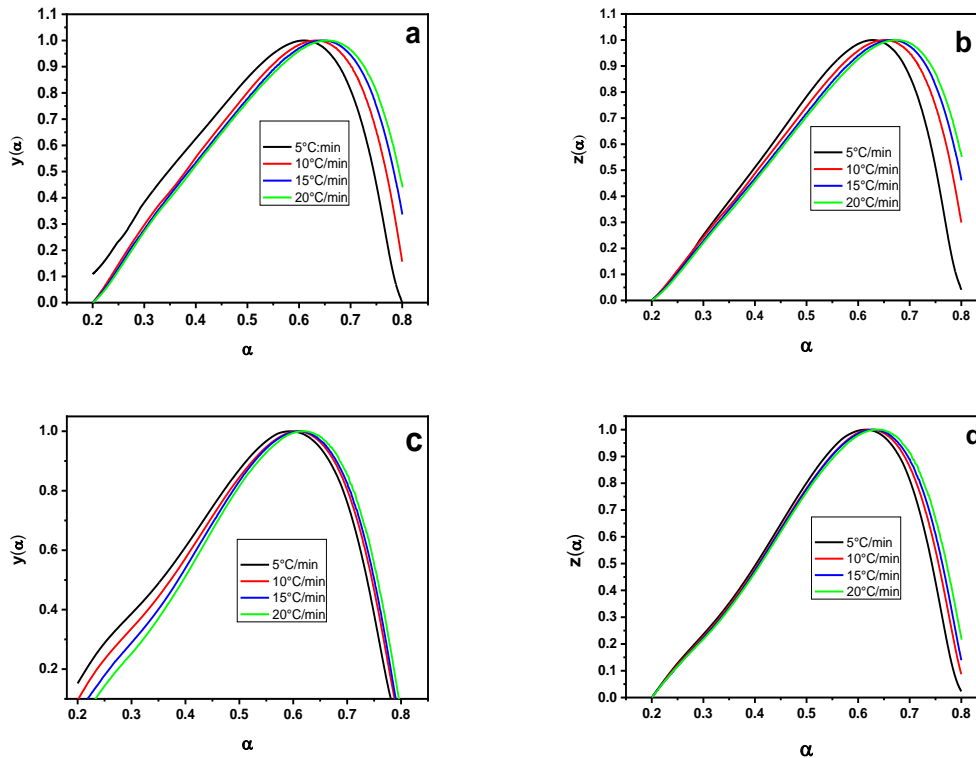

Fig. 5 Plots of composite's A (a, b) and B (c, d) characteristic functions $y(\alpha)$ and $z(\alpha)$

E.F.Assanvo et al   Int. J. Renew. Energy Dev 2024, 13(1), 1-9

| 7

Table 2
A and B Composites $\alpha_{max,y}$, $\alpha_{max,z}$, α_{max}, , $f'(\alpha_{max})$ and Arrhenius pre-exponential factor values for different heating rate β

β	Composite A				Mean Value	Composite B				Mean Value
	5	10	15	20		5	10	15	20	
$\alpha_{max,y}$	0.608	0.637	0.657	0.667	0.642	0.592	0.604	0.617	0.626	0.609
$\alpha_{max,z}$	0.628	0.654	0.676	0.685	0.660	0.614	0.626	0.643	0.648	0.632
α_{max}	0.602	0.650	0,658	0.668	0.644	0.590	0.638	0.610	0.610	0.612
$f'(\alpha_{max})$	-1.540	-1.330	-1.370	-1.260	-1.375	-1.180	-0.970	-1.090	-1.090	-1.082
$A * 10^{15}(min^{-1})$	4.480	4.150	4.320	3.530	4.120	11.14	10.23	10.22	10.12	10.42

composite A than the composite B over the two stages of composites decomposition. The same remarks apply to n values, and inversely to α values for the various heating rates. This suggest that the A composite may be more stable than the B composite. In the second and main stage of decomposition, composite A has the highest calculated activation energy values using Kissinger and FWO. The type and percentage of matrix, as well as the reinforcement loadings, influence material properties such as mechanical properties, thermal stability, rheology properties, and others (Shan *et al.*, 2016). In this study, the more the matrix percentage used in composite elaboration increases, the more the activation energy value decreases and this could be explained by less adhesion of the matrix to the fiber due to the excess of matrix 10% used. In accordance with the studies of Oza *et al.*, (2014) and Rowe *et al.*, (2016) driven about the stability of composite materials, increased bond energy produces higher activation energy with enhances thermal stability. A better knowledge of the thermal deterioration behavior of composites as a result of composite processing can be achieved with the use of the activation energy data. Therefore, from the all above, we can deduce that composite A is more thermally stable than B.

4. Conclusion

Elaborated by compression molding process, the composite materials A and B based on jute fiber undergo two major steps during the degradation process where is being processed at very higher temperatures over the range between 200°C to 550°C shows that the elaborated composites are thermally stable. The apparent activation energy of thermal deterioration was estimated using two-non isothermal methods built on the FWO and Kis singer equations. The findings show that the amount of conversion determines how much this energy is involved, and that the thermal decomposition process disintegrates composites into a number of degradation reaction steps. The JMA model ($n < 1$) was discovered by using the Malek technique to be the ideal decomposition reaction model for the A and B composites and could be established as:

- Composite A: $f_A(\alpha) = 0.48(1-\alpha)[-\ln(1-\alpha)]^{(-1.08)}$

- Composite B: $f_B(\alpha) = 0.5(1-\alpha)[-\ln(1-\alpha)]^{(-1)}$

The calculated values of the pre-exponential factors were respectively for A and B composite materials, $4.12 * 10^{15} min^{-1}$ $10.42 * 10^{15} min^{-1}$; allowing us find out the final equation characterizing the process, then to model the kinetic study and to follow the degradation process of the elaborated composites. By the results analysis, our elaborated composites are both thermally stable, thereafter recapitulative analysis of the parameters, composite A is found to be more thermally stable than composite B. In addition, regarding the big gap between the calculated values of the Arrhenius factor, the possibility of investigating various ratio of blended resin or the effect of fiber treatment into the elaboration of such composite materials have to be taken into account for further studies.

Author Contributions: Edja Assanvo Florentin; supervision, formal analysis, writing—review and editing, and validation, Toure Kicoun Jean-Yves N'Zi: Conceptualization, methodology, data analysis, writing— review original draft, editing, N'Gatta Kanga Marius; review and editing, Boa David; supervision, writing—review and editing, validation. All authors have read and agreed to the published version of the manuscript.

Conflicts of Interest: The authors declare no conflict of interest.

References

Arrakhiz, F. Z., Achaby, M. El, Malha, M., Bensalah, M. O., Fassi-fehri, O., Bouhfid, R., Benmoussa, K., & Qaiss, A. (2013). Mechanical and thermal properties of natural fibers reinforced polymer composites: Doum / low density polyethylene. *Journal of materials and design*, 43, 200–205. https://doi.org/10.1016/j.matdes.2012.06.056 .

Assanvo, E. F., Gogoi, P., Dolui, S. K., & Baruah, S. D. (2015). Synthesis, characterization, and performance characteristics of alkyd resins based on Ricinodendron heudelotii oil and their blending with epoxy resins. *Industrial Crops and Products,* 65, 293–302. https://doi.org/10.1016/j.indcrop.2014.11.049

Assanvo, E. F., Konwar, D., & Baruah, S. D. (2015). Thermal behavior of Ricinodendron heudelotii oil polymer. *Journal of Thermal Analysis and Calorimetry,* 119(3), 1995–2003. https://doi.org/10.1007/s10973-015-4423-5 .

Butler, S. (2018). Contrôle Et Optimisation D'un procédé De Fabrication De Mousses Acoustiques Thermodurcissables à porosité Ouverte (Doctoral dissertation, Ecole Polytechnique, Montreal (Canada)).

Barsoum, I. (2011). Chapter 17. In The Scattered Pearls: A History of Syriac Literature and Sciences (pp. 318-337). Piscataway, NJ, USA:

E.F.Assanvo et al   Int. J. Renew. Energy Dev 2024, 13(1), 1-9

| 8

Gorgias Press. https://doi.org/10.31826/9781463230777-017

Chen, R. S., Ahmad, S., Gan, S., Salleh, M. N., Ab Ghani, M. H., & Mou'ad, A. T. (2016). Effect of polymer blend matrix compatibility and fibre reinforcement content on thermal stability and flammability of ecocomposites made from waste materials. *Thermochimica Acta*, 640, 52-61. https://doi.org/10.1016/j.tca.2016.08.005

Darus, S. A. A. Z. M., Ghazali, M. J., Azhari, C. H., Zulkifli, R., Shamsuri, A. A., Sarac, H., & Mustafa, M. T. (2020). Physicochemical and Thermal Properties of Lignocellulosic Fiber from Gigantochloa Scortechinii Bamboo: Effect of Steam Explosion Treatment. *Fibers and Polymers,* 21(10), 2186–2194. https://doi.org/10.1007/s12221-020-1022-2

Elisabeth, L., Siqueira, V. De, Vaz, B., Benedito, J., & Junior, G. (2018). Soybean waste in particleboard production Aproveitamento de resíduos da soja para a produção de painéis aglomerados. *Agricultural Sciences,* 42(2), 186–194. http://dx.doi.org/10.1590/1413-70542018422015817

Hadiyanto, Christwardana, M., Sutanto, H., Suzery, M., Amelia, D., & Aritonang, R. F. (2018). Kinetic study on the effects of sugar addition on the thermal degradation of phycocyanin from Spirulina sp. *Food Bioscience,* 22, 85–90. https://doi.org/10.1016/j.fbio.2018.01.007

Hamidon, M. H., Sultan, M. T. H., Ariffin, A. H., & Shah, A. U. M. (2019). Effects of fibre treatment on mechanical properties of kenaf fibre reinforced composites: A review. *Journal of Materials Research and Technology*, 8(3), 3327–3337. https://doi.org/10.1016/j.jmrt.2019.04.012

Janković, B., Mentus, S., & Janković, M. (2008). A kinetic study of the thermal decomposition process of potassium metabisulfite: Estimation of distributed reactivity model. *Journal of Physics and Chemistry of Solids,* 69(8), 1923–1933. https://doi.org/10.1016/j.jpcs.2008.01.013.

Kakati, N., Assanvo, E. F., & Kalita, D. (2019). Alkalinization and graft copolymerization of pineapple leaf fiber cellulose and evaluation of physic-chemical properties. *Polymer Composites*, 40(4), 1395-1403. https://doi.org/10.1002/pc.24873

Kakati, N., Assanvo, E. F., & Kalita, D. (2019). Synthesis and Performance Evaluation of Unsaturated Polyester Blends of Resins and Its Application on Non-woven/Fabric Jute Fibers Reinforced Composites. *Journal of Polymers and the Environment*, 27(11), 2540–2548. https://doi.org/10.1007/s10924-019-01537-5.

Keller, A. (2003). Compounding and mechanical properties of biodegradable hemp fibre composites. *Composites Science and Technology,* 63(9), 1307–1316. https://doi.org/10.1016/S0266-3538(03)00102-7

Khachani, M., El Hamidi, A., Halim, M., & Arsalane, S. (2014). Non-isothermal kinetic and thermodynamic studies of the dehydroxylation process of synthetic calcium hydroxide Ca(OH)2. *Journal of Materials and Environmental Science*, 5(2), 615–624.

Khoathane, M. C., Vorster, O. C., & Sadiku, E. R. (2008). Hemp fiber-reinforced 1-pentene/polypropylene copolymer: The effect of fiber loading on the mechanical and thermal characteristics of the composites. *Journal of Reinforced Plastics and Composites*, 27(14), 1533–1544. https://doi.org/10.1177/0731684407086325

Kuranchie, C., Yaya, A., & Bensah, Y. D. (2021). The effect of natural fibre reinforcement on polyurethane composite foams – A review. Scientific African, 11. https://doi.org/10.1016/j.sciaf.2021.e00722.

La Mantia, F. P., & Morreale, M. (2011). Green composites: A brief review. *Composites Part A: Applied Science and Manufacturing*, 42(6), 579–588. https://doi.org/10.1016/j.compositesa.2011.01.017.

Monteiro, S. N., Calado, V., Rodriguez, R. J. S., & Margem, F. M. (2012). Thermogravimetric stability of polymer composites reinforced with less common lignocellulosic fibers - An overview. *Journal of Materials Research and Technology,* 1(2), 117–126. https://doi.org/10.1016/S2238-7854(12)70021-2

Mugdha Bhat, K., Rajagopalan, J., Mallikarjunaiah, R., Nagaraj Rao, N., & Sharma, A. (2022). Eco-Friendly and Biodegradable Green Composites. *IntechOpen.* https://doi.org/10.5772/intechopen.98687

N'Gatta, K. M. N., Belaid, H., Hayek, J. El, Assanvo, E. F., Kajdan, M., Masquelez, N., Boa, D., Cavaillès, V., Bechelany, M., & Salameh, C. (2022). 3D printing of cellulose nanocrystals based composites to build robust biomimetic scaffolds for bone tissue engineering. *Scientific Reports*, 1–14. https://doi.org/10.1038/s41598-022-25652-x.

Nenonene, A. Y., Koba, K., Rigal, L., & Sanda, K. (2014). Development of kenaf's particleboards agglomerated with produced tannins by some plant organs from togo. *Sciences de la vie, de la terre et agronomie,* 02(1), 36-40; http://publication.lecames.org/index.php/svt/article/viewFile/94/174

Oza, S., Ning, H., Ferguson, I., & Lu, N. (2014). Effect of surface treatment on thermal stability of the hemp-PLA composites: Correlation of activation energy with thermal degradation. *Composites Part B: Engineering*, 67, 227–232. https://doi.org/10.1016/j.compositesb.2014.06.033 .

Raju, G. U., & Kumarappa, S. (2012). Experimental study on mechanical and thermal properties of epoxy composites filled with agricultural residue. *Polymers from Renewable Resources*, 3(3), 117–138. https://doi.org/10.1177/204124791200300303

Rangappa, S. M., Siengchin, S., Parameswaranpillai, J., Jawaid, M., & Ozbakkaloglu, T. (2022). Lignocellulosic fiber reinforced composites: Progress, performance, properties, applications, and future perspectives. *Polymer Composites*, 43(2), 645-691, https://doi.org/10.1002/pc.26413 .

Reis, R. H. M., Nunes, L. F., Oliveira, M. S., De Veiga Junior, V. F., Filho, F. D. C. G., Pinheiro, M. A., Candido, V. S., & Monteiro, S. N. (2020). Guaruman fiber: Another possible reinforcement in composites. *Journal of Materials Research and Technology*, 9(1), 622–628. https://doi.org/10.1016/j.jmrt.2019.11.002 .

Reis, R. S., Tienne, L. G. P., Souza, D. de H. S., Marques, M. de F. V., & Monteiro, S. N. (2020). Characterization of coffee parchment and innovative steam explosion treatment to obtain microfibrillated cellulose as potential composite reinforcement. *Journal of Materials Research and Technology,* 9(4), 9412–9421. https://doi.org/10.1016/J.JMRT.2020.05.099 .

MaÂlek, J. (2000). Kinetic analysis of crystallization processes in amorphous materials. *Thermochimica Acta*, 355(1–2), 239–253. https://doi.org/https://doi.org/10.1016/S0040-6031(00)00449-4

Rosa, M. F., Chiou, B., Medeiros, E. S., Wood, D. F., Williams, T. G., Mattoso, L. H. C., Orts, W. J., & Imam, S. H. (2009). Bioresource Technology Effect of fiber treatments on tensile and thermal properties of starch / ethylene vinyl alcohol copolymers / coir biocomposites. *Bioresource Technology,* 100(21), 5196–5202. https://doi.org/10.1016/j.biortech.2009.03.085

Rowe, A. A., Tajvidi, M., & Gardner, D. J. (2016). Thermal stability of cellulose nanomaterials and their composites with polyvinyl alcohol (PVA). *Journal of Thermal Analysis and Calorimetry*, 126(3), 1371–1386. https://doi.org/10.1007/s10973-016-5791-1 .

Sahin, A., Tasdemir, H. M., Karabulut, A. F., & Gürü, M. (2017). Mechanical and Thermal Properties of Particleboard Manufactured from Waste Peachnut Shell with Glass Powder. *Arabian Journal for Science and Engineering,* 42(4), 1559–1568. https://doi.org/10.1007/s13369-017-2427-0 .

Scatolino, M. V., Costa, A. de O., Guimarães Júnior, J. B., Protásio, T. de P., Mendes, R. F., & Mendes, L. M. (2017). Eucalyptus wood and coffee parchment for particleboard production: Physical and mechanical properties. *Ciência e Agrotecnologia*, 41(2), 139–146. https://doi.org/10.1590/1413-70542017412038616.

Singh, H., Inder, J., Singh, P., Singh, S., Dhawan, V., & Tiwari, S. K. (2018). A Brief Review of Jute Fibre and Its Composites Harpreet. *Materials Today: Proceedings*, 5(14), 28427–28437. https://doi.org/10.1016/j.matpr.2018.10.129

Svoboda, R., & Málek, J. (2011). Interpretation of crystallization kinetics results provided by DSC. *Thermochimica Acta,* 526(1–2), 237–251. https://doi.org/10.1016/j.tca.2011.10.005 .

Tajvidi, M., & Takemura, A. (2010). Thermal degradation of natural fiber-reinforced polypropylene composites. Journal of *Thermoplastic Composite Materials*, 23(3), 281–298. https://doi.org/10.1177/0892705709347063

Thiruchitrambalam, M., Athijayamani, A., Sathiyamurthy, S., & Thaheer, A. S. A. (2010). A review on the natural fiber-reinforced polymer composites for the development of roselle fiber-reinforced polyester composite. *Journal of Natural Fibers*, 7(4), 307-323. August 2014, 37–41. https://doi.org/10.1080/15440478.2010.529299 .

Tserki, V., Matzinos, P., Zafeiropoulos, N. E., & Panayiotou, C. (2006). Development of biodegradable composites with treated and compatibilized lignocellulosic fibers. Journal of applied polymer science, 100(6), 4703-4710. https://doi.org/10.1002/app.23240

Vyazovkin, S. (2020). Kissinger Method in Kinetics of Materials: Things to Beware and Be Aware of. *Molecules,* 25(12). https://doi.org/10.3390/molecules25122813 .

Vyazovkin, S., Burnham, A. K., Criado, J. M., Pérez-Maqueda, L. A., Popu, C., & Sbirrazzuoli, N. (2011). ICTAC Kinetics Committee recommendations for performing kinetic computations on thermal analysis data. *Thermochimica Acta,* 520(1–2), 1–19. https://doi.org/10.1016/j.tca.2011.03.034.

Yakout, M., & Elbestawi, M. A. (2017). Additive Manufacturing of Composite Materials : An Overview. 6th International Conference on Virtual Machining Process Technology (VMPT), Montréal, May, 1–8. https://www.researchgate.net/profile/Mostafa-Yakout/publication/316688880_Additive_Manufacturing_of_Composite_Materials_An_Overview/links/590c9667458515978182e951/Additive-Manufacturing-of-Composite-Materials-An-Overview.pdf

Zafeiropoulos, N. E., Baillie, C. A., & Hodgkinson, J. M. (2002). Engineering and characterisation of the interface in flax fibre/polypropylene composite materials. Part II. The effect of surface treatments on the interface. *Composites Part A: Applied Science and Manufacturing,* 33(9), 1185–1190. https://doi.org/10.1016/S1359-835X(02)00088-X